Food Chemistry: Molecular Sciences 6 (2023) 100158

Contents lists available at ScienceDirect

Food Chemistry: Molecular Sciences

journal homepage: www.sciencedirect.com/journal/food-chemistry-molecular-sciences

Thermal and pH stability of *Justicia spicigera* (Mexican honeysuckle) pigments: Application of mathematical probabilistic models to predict pigments stability

Oscar Jiménez-González [1], Aurelio López-Malo, Julio Emmanuel González-Pérez, Nelly Ramírez-Corona, José Ángel Guerrero-Beltrán [*,2]

Departamento de Ingeniería Química, Alimentos y Ambiental, Universidad de las Américas Puebla. Ex hacienda de Santa Catarina Mártir, C.P. 72810, San Andrés Cholula, Puebla, Mexico

A R T I C L E I N F O

Keywords:
Mexican honeysuckle (*Justicia spicigera*)
Peonidin
Anthocyanins
Pigments degradation
Color stability
Time-to-failure model

A B S T R A C T

Kinetic and probabilistic (Time-to-Failure, TTF) models were used to predict the color (L^*, a^*, b^* total color differences (ΔE), *Hue* and *Chroma*) stability of *Justicia spicigera* leaves pigments subjected to different temperatures (40 – 80 °C) and pHs (2 – 12). The change in pH caused different hues (from 60° = orange red to 268° = deep-blue) due to the shift effect of anthocyanins in the extract. Temperatures higher than 60 °C increased the color degradation. High heat sensitivity was observed at pH 4 (Ea = 90.27) and 10 (Ea = 154.99 kJ/mol). The Time-to-Failure model for both ΔE and *Hue* describes the effect of pH and temperature in the *J. spicigera* extracts. High pHs and temperatures applied to the extracts increased the probability of showing $\Delta Es > 4$ or *Hue* changes over 20 %. Nearby the neutral region of pH, pigments of *J. spicigera* were more stable. The TTF model might be a useful tool to describe and predict the behavior of pigments added to foods.

1. Introduction

Today, the use of natural pigments in the food industry has increased. The addition of colorants or pigments to foods may influence their appearance, and the decision and purchase intention by consumers. Natural pigments, such as carotenoids, chlorophylls, betalains and anthocyanins have shown multiple health benefits due to their antioxidant characteristics (Rodriguez-Amaya, 2016; Rodriguez-Amaya 2019). Anthocyanins, important water soluble-colored-harmless flavonoids (Rajan et al., 2018), are found in many fruits, vegetables and flowers. Anthocyanins can be found in red, purple or blue colors (Khoo et al., 2017). This characteristic makes anthocyanins to be potential natural pigments for foods and beverages. However, anthocyanins are unstable to physical and chemical factors such as pH, temperature, oxygen, light, enzymes, sugars, co-pigments, among other factors (Ahmed et al., 2002; Cevallos-Casals & Cisneros-Zevallos, 2004; Gençdağ et al., 2022; Rajan et al., 2018). Moreover, temperatures and pH are the most important factors in color stability because the structure of the molecule may change (Liu et al., 2018; Loypimai et al., 2016; Roobha et al., 2011). Temperature could destroy the anthocyanin when this increase (Liu et al 2018). On the other hand, pH affects the structure of the molecules which leads in distinct colors (Rakić & Poklar Ulrih, 2021). However, some of the anthocyanin forms are highly unstable and tend to lose their color.

Justicia spicigera (Mexican honeysuckle) is a shrub which has been used since pre-Hispanic (before the Hispanic conquest) times in America for coloring textiles or crafts; it has shown also multiple health benefits (Baqueiro-Peña & Guerrero-Beltrán, 2017). Decoction of leaves in water results in a pink-purple color extract that is rich in different polyphenols, including anthocyanins (Awad et al., 2015) which once concentrated it turns into a deep blue color. These pigments could be used as natural colorants due to their wide range of hues (from red to blue) (Rajan et al., 2018). Recently, the *Justicia spicigera* pigments were used to increase bioactive compounds and for coloring purposes in “tortillas” of maize (flat Mexican bread) (Alvarez-Poblano et al., 2020). In other study, pigments were added to yogurt and jelly to obtain functional foods with attractive color (Castro-Alatorre et al., 2021). Also, pigments were encapsulated by spray drying to increase its stability and preserve

* Corresponding author.
E-mail address: angel.guerrero@udlap.mx (J.Á. Guerrero-Beltrán).
[1] ORCID: 0000-0001-5445-5033.
[2] ORCID: 0000-0002-5440-6677.

https://doi.org/10.1016/j.fochms.2022.100158
Received 5 August 2022; Received in revised form 5 December 2022; Accepted 11 December 2022
Available online 13 December 2022

bioactive compounds (Pavón-García et al., 2011; Castro-Alatorre et al., 2021; Jiménez-González & Guerrero-Beltrán, 2022).

Almost all food processing procedures require thermal treatment at certain point for: inactivate microbials or reduce microbial loads, remove water, inactivate enzymes, generate physical or chemical changes to deliver edible safe foods to consumers (Liao et al., 2019; Oancea, 2021). However, during thermal processing, the color of the food or beverage may change, be reduced or be lost, just to mention some changes. Therefore, the color standardization of foods is an essential step in the foods production. Generally, isothermal treatments are used to obtain experimental data with the intention of determining kinetic parameters of degradation factors in foods and relate them to other characteristics, such as quality (Ahmed et al., 2002). The color degradation data, in general, fits to a zero or first order kinetics; that has been studied for a number of researchers (Oancea, 2021); however, results do not give accurate information when a product should be rejected due to low quality factors such as inappropriate color. Survival microbial analysis, based on the Weibull model, was introduced by Gacula & Singh (1984); they estimated the time when a food product should be rejected based on stablished parameters. The model has been also applied to describe the influence of extrinsic factor throughout the time for detecting spoilage microorganisms in foods (Kosegarten et al., 2017) or for predicting the shelf life of different dairy, meat, cereal fruit, and vegetable based food products (da Silva Simão et al., 2022; Jacobo-Velázquez et al., 2010; Marques et al., 2020; Rasane et al., 2015). Based on the previous information, survival analysis could be used as tool to predict the lifetime/stability of pigments when are submitted to different conditions during processing of a food.

Considering that anthocyanins are in current use, this work hypothesized that mathematical methods could be used as a useful tool to predict the lifetime of *J. spicigera* pigments. Thus, the aim of this work was to evaluate the viability time of *J. spicigera* pigments when subjected to different pHs and temperatures using first order kinetics and Time-to-Failure models.

2. Materials and methods

2.1. Extraction and powder of pigments

The *Justicia spicigera* extracts were obtained from dried grounded leaves (from the same cultivar acquired with local producer at Puebla, Mexico, in March 2019) according to the Baqueiro-Peña & Guerrero-Beltrán (2017) methodology with some modifications. The extraction consisted in macerating the leaves powder with 50 % ethanol (PubChem CID: 702) solution at 1:83.33 ratio (w/v) for 2 h in dark conditions. The mixture was then centrifugated using a centrifuge model Z 326 K (HERMLE Labortechnik GmbH, Wehingen, Germany) at 6000 rpm (4 °C) for 10 min. The extract was concentrated using a rotatory evaporator (Büchi R-300, Büchi Labortechnik AG, Flawil, Switzerland) at 45 °C and 54 mmHg until getting one third part of the initial volume. Therefore, the concentrated extract was mixed with 5 % (w/v) maltodextrin (PubChem CID: 68229136), placed in polyethylene bags, and then frozen at −80 °C for later lyophilization using a LABCONCO freeze dryer (FreeZone, Kansas, USA) at 0.133 mmHg (-50 °C and 25 °C in the condenser and chamber temperatures, respectively) for 48 h. The lyophilized extract of *J. spicigera* was ground to get a fine powder, keep in sealed plastic tubes and maintained in a desiccator at room temperature until use.

2.2. Solution at different pHs

To obtain different colors, 0.1 g of powder was dissolved in 50 mL of McIlvaine buffer (citric acid (PubChem: 311); sodium phosphate dibasic (PubChem: 24203) of different pHs (2, 4, 8) in glass test tubes with plastic caps. Solutions of powders at pH 10 and 12 were adjusted with 1 M sodium hydroxide (PubChem: 14798). All samples were left at room temperature for 1 h.

2.3. Color of solutions

A Multiskan SkyHigh microplate spectrophotometer (Thermoscientific, Singapore, Singapore) was used for color determination. The whole visible spectrum (400 – 800 nm) was scanned at constant intervals ($\Delta\lambda = 1$ nm) using a 96-wells microplate and distilled water as reference. *CIELab** color parameters were calculated following the spectrophotometric method proposed by APHA et al. (1992) with some modifications. Briefly, transmittance values were recorded for 30 different wavelengths (λ) for the *X*, *Y* and *Z* tristimulus values. The *X*, *Y* and *Z* tristimulus values were calculated using Eq. (1).

$$X, YorZ = \sum_{\lambda} T\%(\lambda) \times F \tag{1}$$

where *T%(λ)* is the transmittance value at each wavelength and *F* is the value for each tristimulus value: $X = 0.03269$, $Y = 0.03333$, and $Z = 0.03938$.

To convert the *X*, *Y* and *Z* tristimulus values to *L** (lightness), *a** and *b** color parameters, Eqs. (2), (3), and (4) were used, respectively.

$$L^* = 116^*\left(\frac{Y}{Y_n}\right) - 16 \tag{2}$$

$$a^* = 500\left[\left(\frac{X}{X_n}\right)^{\frac{1}{3}} - \left(\frac{Y}{Y_n}\right)^{\frac{1}{3}}\right] \tag{3}$$

$$b^* = 200\left[\left(\frac{Y}{Y_n}\right)^{\frac{1}{3}} - \left(\frac{Z}{Z_n}\right)^{\frac{1}{3}}\right] \tag{4}$$

where X_n, Y_n and Z_n are 98.041, 100.000 and 118.103, respectively, for a C illuminant 2° observer, and X/X_n, Y/Y_n and $Z/Z_n > 0.01$.

The *L**(black (0)-white (100)), *a** (red-green), and *b** (yellow-blue) color parameters were used to calculate *Hue* (H°), *Chroma* (C) and the total change in color (ΔE) with equations (5), (6), and (7), respectively.

$$Hue = \tan^{-1}\left(\frac{b^*}{a^*}\right) \tag{5}$$

$$Chroma = \sqrt{a^{*2} + b^{*2}} \tag{6}$$

$$\Delta E = \sqrt{\left(L^* - L_o^*\right)^2 + \left(a^* - a_o^*\right)^2 + \left(b^* - b_o^*\right)^2} \tag{7}$$

where L_o^*, a_o^* and b_o^* are the color parameters at time zero and *L**, *a** and *b** color parameters at any time.

2.4. Color thermal stability

The thermal stability of color was evaluated at three temperatures (40, 60 and 80 °C). For each temperature, all pH solutions were placed in a Büchi B-300 thermoelectric water bath (Büchi Labortechnik AG, Flawil, Switzerland). An aliquot of each sample was taken at one-hour intervals for seven hours (0, 60, 120, 180, 240, 300, 360, 420 min). Samples were cooled down in an ice-water to stop the thermal effect. *Hue* values were taken as the most feasible indicator of color degradation. Hue values were taken as the most reliable indicator of color degradation. Some researchers have pointed out that Hue can be a sensitive parameter for color changes in response to temperature (Swain et al., 2014) and it can be easily calculated or given by any colorimeter device calculated by the software (Cantrell et al 2010). First-order kinetics, at constant temperature, in terms of fractional conversion (Ahmed et al., 2002), was performed using Eq. (8).

$$\frac{C_t - C_E}{C_0 - C_E} = exp^{-kt} \tag{8}$$

where C_t, C_0, and C_E are the *Hue* values at time *t*, zero time and infinite time, respectively; *k* is the constant rate (min^{-1}), and *t* the heating time (min).

To determine the degradation rate at different temperatures, the Arrhenius equation (Loypimai et al., 2016) was used: Eqs. (9) and (10).

$$k = k_0 exp\left(\frac{-E_a}{RT}\right) \tag{9}$$

$$\ln k = \ln(ko) - \left(\frac{E_a}{R}\right)\left(\frac{1}{T}\right) \tag{10}$$

where k_0 is the frequency factor (min^{-1}), E_a is the activation energy (kJ/mol), *R* is the universal gas constant (8.314 J/mol K), and *T* is the absolute temperature (K).

A plot of experimental data of ln *k* vs *1/T* might render a straight line with slope E_a/R (to determine E_a). As pigments stability is sensitive to temperature, Q_{10} values were calculate using Eq. (11).

$$Q_{10} = \frac{k_2}{k_1} \tag{11}$$

where k_1 and k_2 are the constant rates at temperature T_1 and T_2 ($T_2 = T_1 + 10\ ^\circ C$), respectively, and Q_{10} (temperature coefficient) is dependance of temperature of a process.

2.5. Time-to-Failure (TTF) prediction

The Time-to-Failure (TTF) model is a statistical tool based on the Weibull distribution model (Zhai et al., 2013). It uses time series data of the failures of a product to fit a parametric distribution. It can give valuable information for optimizing the life cycle of a product (Zhai et al., 2013). It provides the probability for observing Time-to-Failure values; therefore, the failure time (in minutes) can be defined as shelf life (Kosegarten et al., 2022) of the food product. Based on the time where changes occur at least at 20 % of *Hue* (Hue_{20}, %) or at ΔE values greater or equal to 4, a polynomial model that describe both Hue_{20} and ΔE changes can be used (12).

$$Ln(TTF) = \beta_0 + \beta_x x + \beta_y y + \beta_{xy} xy + \beta_{xx} x^2 + \beta_{yy} y^2 \tag{12}$$

where *TTF* is the time when Hue_{20} or ΔE presents a change, considered a failure; β_{ij} are the coefficients of the polynomial model, *x* and *y* are the normalized values (normalized value = (value – average)/standard deviation) of the studied factors (pH and temperature values, respectively). All variables and interactions were used to build the *TTF* model.

2.6. Statistical analysis

Extraction of *Justicia spicigera* were made in duplicate. pH adjustment, thermal stability and color determination were made in triplicate for each obtained extract. Results are reported as averages with standard deviation. Data were subjected to an analysis of variance (ANOVA) using the Statistix 8.1 (Analytical Software, Tallahassee, FL, USA) program. To determine differences within samples ($p \leq 0.05$), the Tukey test was conducted. The Time-to-Failure regression model was obtained using the Minitab 16 (Minitab Inc., State College, PA., USA) software.

3. Results and discussion

3.1. Color of solutions at time zero

The initial color of the solution before lyophilization was a deep bluish-purple color. Once dissolved without pH adjustment, the solution was lighter in color: $L^* = 80.26 \pm 0.26$, $a^* = 1.88 \pm 0.09$, $b^* = -5.69 \pm 0.13$, *Chroma* $= 5.99 \pm 0.15$, *Hue* $= 288.30 \pm 0.61$ and $\lambda^{max} = 590$. The color parameters values of the *J. spicigera* solutions at different pHs are shown in Table S1. The initial colors observed in solutions of *J. spicigera* adjusted at different pHs were: 60.4 ± 0.48 (orange red) and 59.56 ± 0.44) (red–orange) for pHs 2 and 4, respectively, located in the first quadrant (red to yellow tones) of the color wheel with a^* and b^* positive values. Th increase of pH in solutions (pH 8 and 10), purple (296.28 ± 0.05), bluish-purple (275.59 ± 0.27) colors were observed, respectively. These colors are in the fourth quadrant of the color wheel (blue to red hues), showing positive a^* and negative b^* values. Finally, for alkaline pH (12), a deep blue color was observed (268.15 ± 0.83), values located in the third quadrant (green to blue hues) of the color wheel, with both a^* and b^* negative values.

Changes in color were observed, due to pH changes, by other authors for different types of anthocyanins (Khoo et al., 2017; Rakić & Poklar Ulrih, 2021). It has been reported that *J. spicigera* contain at least twelve different types of anthocyanins, being peonidin 3,5-diglucoside and malvidin 3,5-diglucoside the most abundant anthocyanins (Awad et al., 2015). Peonidin is stable at alkaline pHs, showing blue colors (Rajan et al., 2018). The blue colors of some flower that growth in alkaline soils is due to the presence of peonidin (Rajan et al., 2018). On the contrary, peonidin show a red-purplish color in fruits of low pH; this explain the changes observed in the extracts at different pHs.

Color can be described as the way of how the light is absorbed and transmitted through a medium. Therefore, wavelengths with maximum absorption (λ^{max}) in the visible ranges of the electromagnetic spectrum show colors. Changes in the UV–vis spectrum are related to the changes in molecular structure due to pH variations. Fig. 1 shows the spectra of *J. spicigera* solutions adjusted to pHs 2, 4, 8, 10, and 12.

Rajan et al. (2018) have pointed out that at low pHs (1, 2, and 4), the quinoidal base form is predominant. In Fig. 1, at both pHs 2 (Fig. 1a) and 4 (Fig. 1b), maxima absorbances were observed at wavelengths of 471 and 487 nm (Table S1), respectively, corresponding to the absorption in the blue-green region of the electromagnetic spectrum: observed as red by the human eye. An orange-red pale color was close to 60° of *Hue* (Table S1). As pH decreases, the chroma or saturation decreases as well.

The color of the *J. spicigera* solution at pHs around neutral values (≈ 8) was a bluish-purple color, with a maximum absorbance of 589 nm (Fig. 1c, Table S1). At this pH, the formation of chalcones and some quinoidal bases are predominant in peonidin (Rajan et al., 2018). Other anthocyanins such as malvidin shows the anionic quinoidal base form at this pH (Habtemariam, 2019). Other authors have point out that the presence of multiples anthocyanins in different concentrations in molecular form, glycosylated, acylated), or isomers might influences in the final color (Moreno & Peinado, 2012), which could explain the final purple color of the solution.

As pH is adjusted to basic conditions (pHs 10 and 12), the hue of the solution turn into a deep blue color (λ≈ 589.5) (Fig. 1d and 1e); however, a slight reduction in chroma and lightness (Table S1) is observed. At these pHs, the predominant form of most anthocyanins is the chalcones one. However, for peonidin, both quinoidal bases and chalcones form may exist in alkaline solutions (Rajan et al., 2018), showing bluish-purple and blue hues, respectively.

3.2. Color changes dur to pH and temperature

The thermal degradation of *J. spicigera* pigments was studied at 40, 60 and 80 °C. Changes in color were observed in the a^* and b^* color parameters, corresponding to green–red and blue-yellow in the color space, respectively. Fig. 2 (Table 1) shows the effect of temperature on the *J. spicigera* solutions at different pHs. Large dispersion of the points indicates a large change in color in comparison to the color at time zero (Fig. 2 a-c). Color changes take different trends, depending on the pH (Fig. 2 a-c):

i) At pH 2 (Fig. 2, Table 1), changes of color in the *J. spicigera* extract were less evident, especially at 40 °C. The values of the a^* color parameter were between 2 and 4. The values of the b^* color parameter were between 5 and 8. A slight decrease in the a^* color parameter

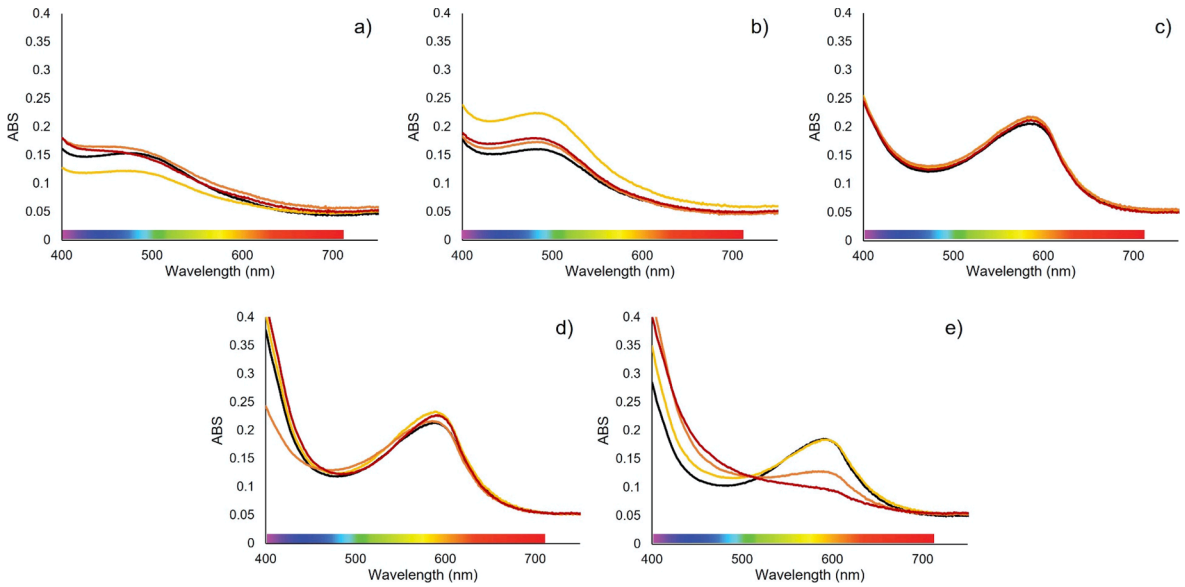

Fig. 1. Effect of pH and temperature (°C) on the visual spectra (400 – 750 nm) of *Justicia spicigera* solutions at different pHs: a) 2, b) 4, c) 8, d) 10, e) 12 and temperatures (after 420 min): 40 °C (yellow line), 60 °C (orange line) and (red line) 80 °C (red line). The black line corresponds to the initial spectra just after pH adjustment at room temperature. (For interpretation of the references to color in this figure legend, the reader is referred to the web version of this article.)

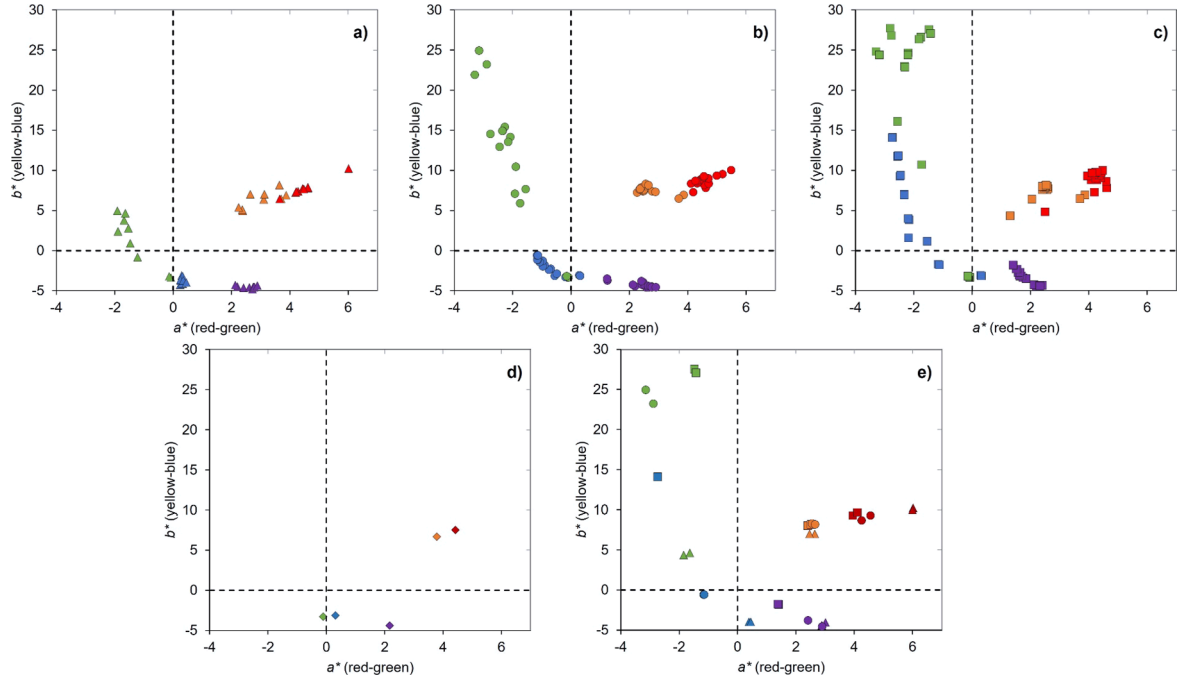

Fig. 2. Evolution of color (a^* vs b^*) as effect of pH on the *J. spicigera* solutions: pH 2 (▲●■), 4 (▲●■), 8 (▲●■), 10 (▲●■), 12 (▲●■) and temperatures a) ▲ 40, b) ● 60, c) ■ 80 °C. The closer the points in the plot, lower degradation of color was observed. d) Initial and e) final values was plotted separately for better visualization.

occurred with a non-significant difference ($p > 0.05$) within temperatures; however, significant difference ($p < 0.05$) was observed regarding the initial color (Fig. 2d, Table S1), indicating a reduction of red color. On the contrary, the b^* color values increased, particularly in *J. spicigera* solutions treated at 60 and 80 °C; however, non-significant changes ($p > 0.05$) were observed in the solution treated at 40 °C. As a result of the change in the UV–vis spectrum, the treatment at 40 °C induced a hypochromic effect or loss in color. In solutions treated at 60 and 80 °C (Fig. 1a), an hyperchromic effect and a bathochromic shift were induced which could be due to the deprotonation of phenolic compounds and the formation of chalcones which color is red-brown (Ngamwonglumlert et al., 2020; Roobha et al., 2011; Sadilova et al., 2006).

ii) Color changes in the *J. spicigera* extract at pH 4 (Fig. 2, Table 1) were like those at pH 2. A reduction in a^* (only significant ($p < 0.05$) for

Table 1
Final values of color parameters of *J. spicigera* extracts adjusted a different pHs after processing 420 min at different temperatures.[a]

T (°C)	pH	*L**	*a**	*b**	*Chroma*	*Hue* (°)	*ΔE* [b]
	2	89.44 ± 0.62bA	2.58 ± 0.11cA	7.00 ± 0.00bB	7.46 ± 0.04bB	69.81 ± 0.76 dB	2.25
	4	88.13 ± 0.18bB	6.01 ± 0.01aA	10.12 ± 0.17aA	11.77 ± 0.15aA	59.29 ± 0.36eC	4.20
40	8	85.65 ± 0.23cA	2.77 ± 0.08bA	−4.52 ± 0.20 dB	5.30 ± 0.12cA	301.58 ± 1.98aAB	1.14
	10	84.94 ± 0.09cB	0.43 ± 0.04dA	−3.99 ± 0.01dC	4.02 ± 0.00 dB	276.09 ± 0.53bA	1.26
	12	89.98 ± 0.37aA	−1.92 ± 0.12eA	4.63 ± 0.17cC	4.83 ± 0.11cB	110.84 ± 1.99cA	8.85
	2	89.59 ± 1.02aA	2.62 ± 0.07bA	8.2 ± 0.09bA	8.6 ± 0.07bA	72.28 ± 0.63dAB	2.58
	4	90.21 ± 0.17aA	4.42 ± 0.21aB	8.94 ± 0.42bA	9.97 ± 0.47bB	63.71 ± 0.03eB	1.64
60	8	85.44 ± 1.16bA	2.67 ± 0.34bA	−4.21 ± 0.54 dB	4.99 ± 0.64cA	302.36 ± 0.00aB	0.77
	10	87.78 ± 0.28abA	−1.14 ± 0.02cB	−0.62 ± 0.01cB	1.3 ± 0.01dC	208.7 ± 0.79bB	3.52
	12	87.78 ± 0.34abB	−3.01 ± 0.19 dB	24.04 ± 1.22aB	24.23 ± 1.23aA	97.12 ± 0.08cB	27.50
	2	91.65 ± 0.13aA	2.48 ± 0.08bA	8.04 ± 0.1dA	8.41 ± 0.12dA	72.87 ± 0.33dA	1.92
	4	90.33 ± 0.00bA	4.04 ± 0.11aB	9.44 ± 0.27cA	10.27 ± 0.29cB	66.86 ± 0.01eA	2.09
80	8	86.35 ± 0.17cA	1.41 ± 0.01cB	−1.82 ± 0.02eA	2.3 ± 0.02eB	307.75 ± 0.14aA	2.71
	10	84.97 ± 0.09 dB	−2.72 ± 0.01eC	14.07 ± 0.04bA	14.33 ± 0.03bA	100.96 ± 0.03bC	17.51
	12	85.54 ± 0.10eC	−1.44 ± 0.04dA	27.28 ± 0.33aA	27.32 ± 0.33aA	93.03 ± 0.05cB	30.70

[a] Lowercase letter in the same column for the same temperature indicate not significant difference ($p < 0.05$) within pH. Uppercase letter in the same column for the same pH indicate not significant difference ($p < 0.05$) within temperature. [b] *ΔE* values were calculates using the values of Table 1 for each pH.

40 °C) and an increase in intensity in *b** color parameters (significant ($p < 0.05$) for all temperatures) were observed. These changes are the result of an increased absorption in the UV–vis spectrum (Fig. 1b), causing an hyperchromic effect. This effect could be probably due to the formation of anthocyanins complexes with other compounds, which lead to the formation of colored molecules (Gençdağ et al., 2022), or the formation of red-brown chalcones. The increase in temperature also may lead to the degradation of the anthocyanins structures (Oancea, 2021; Roobha et al., 2011; Sadilova et al., 2006) causing a possible deglycosylation and a cleavage of the molecule (Patras et al., 2010).

iii) The color of the *J. spicigera* solutions at pH 8 (Fig. 2, Table 1) was the most stable of all pHs. Contrary to other types of anthocyanins such as cyanidin, delphinidin and pelargonidin, peonidin has high stability at neutral pH or even higher (Khoo et al., 2017; Rajan et al., 2018). Changes in the *a** and *b** color parameters (Table 1) were greater in the solution treated at 80 °C: from 2.17 (Table S1) to 1.41 (Table 1) and −4.39 (Table S1) to −1.82 (Table 1), respectively; however, *Hue* remains close to 300° which corresponds to a purple color. A slight change was observed in the spectra (Fig. 1c), almost overlapped, showing that at this pH the change in color was minimal, as a result, at this treatment pigments of solutions was the most thermoresistant.

iv) pHs 10 and 12 had similar effect in the *J. spicigera* solutions. The initial values of color parameters (Fig. 2d, Table S1) were in the fourth quadrant (red-blue) of the color space; after the thermal treatment, the *a** and *b** color parameters changed to the third (blue-green) and second quadrant (green-yellow) (Fig. 2e, Table 1) of the color wheel. The color of the solution with pH 10 treated at 40 °C remained relatively unaffected (Fig. 2a, Tables S1, 1). In solutions treated at 60 and 80 °C (Fig. 2 b-c), the color changed to a pale blue and brownish yellow, respectively. Finally, in the solution at pH 12, color changed drastically at the three experimental temperatures, particularly at 60 and 80 °C (Fig. 2c and e, Table 1). In the solution treated at 80 °C (Table 1), the final color was brownish yellow (*Hue* = 93.03 ± 0.05°) showing high chroma value (27.32 ± 0.33). For the solution treated at 60 °C, *Hue* and chroma were 97.12° and 24.23, respectively (Table 1). The UV–vis spectrum showed an increase in absorbances near 400 nm and a clear reduction of 600 nm (λ^{max}) (Fig. 1e, Table S1). According to the spectrum, an increase in absorbance in the UV region, might result the formation of degraded colorless compounds (Ngamwonglumlert et al., 2020).

3.3. Effect of temperature on color

The *Hue* changes of the *J. spicigera* solutions, adjusted at different pHs, followed a fractional first-order reaction (Fig. 3a); this behavior assumes that the sample reach an equilibrium and not a complete degradation of the evaluated compounds, which was observed for the first time by Speers et al. (1987) in the color degradation of strawberry juice. Recently, in agreement with other studies, it was demonstrate how pigments/visual color degradation follows a fractional first-order kinetics in the degradation of papaya puree carotenoids and visual color (Ahmed et al., 2002), in the polyphenols content of different teas

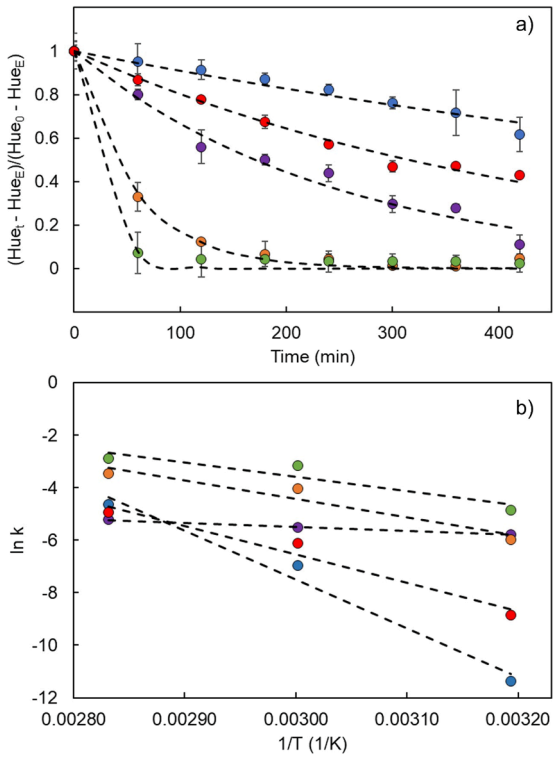

Fig. 3. A) first order *Hue* degradation kinetics of *J. spicigera* solutions at different pHs: pH 2 (●), 4 (●), 8 (●), 10 (●), 12 (●) during heat treatment at 60 °C (mild temperature). b) Arrhenius plot for dependence of degradation rate constants for *Hue*.

(Shannon et al., 2017), and in the degradation of anthocyanins in merlot and ruby grapes (Muche et al., 2018). Fig. 3a clearly shows the effect of pH on the *Hue*. Samples at pH 4, 8 and 10 treated at 60 °C were the most stable since less changes in color, with respect to the initial *Hue*, were observed. Same trends were observed in solutions treated at all temperatures. Changes in *Hue* were greater in solutions treated at high temperatures with exception of the solution at pH 8, which remain almost unchanged as can be observed in Fig. 3b (effect of temperature on the degradation rate constant) and Table 2. This stability in color could be related to the structure of the molecule (quinoidal bases), predominant at pH 8. Also, the stability of peonidin might be the result of the substitution pattern of the "b" benzene ring in the molecule of peonidin; the ring do not include hydroxyl groups to each other in ortho position (Cabrita et al., 2000). Previous studies have shown that the stability of mono-acylated anthocyanins (petanin) could increase at basic pH, specially at pH 8.1 (Fossen et al., 1998).

The regression parameters of the first order kinetics are shown in Table 2. The determination coefficients (R^2) were in the range 0.891 – 0.999. The changes in color of solutions with pH 4 and 10 treated at 40 °C, were not significant ($p > 0.05$) compared to the initial values; from that, kinetic values were calculated and used to calculate the activation energy (E_a) and Q_{10} values.

Table 2 shows the linear regression parameters of color changes (only for *Hue*) after heating the *J. spicigera* extracts for 420 min. A clear increase of *k* values is observed with the increase in temperature at the same pH. Same behavior was observed previously by other authors in the degradation the anthocyanins of black rise bran (Loypimai et al., 2016). For solutions with pH 2 and 12, higher *k* values were observed, specially over 60 °C, indicating low stability at these conditions, and high sensitivity to temperature. Lower *k* values were observed for solutions at pH 4 compared to pH 2. Cevallos-Casals & Cisneros-Zevallos, (2004) found that anthocyanins of sweet potato and purple carrot had higher stability at pH 1 than at pH 3. However, the anthocyanins degradation was mainly due to the temperature effect, causing deglycosylation, nucleophilic attack of water, cleavage, and polymerization (Rodriguez-Amaya, 2019). In solutions with pH 8, the color changes were minimal: *Hue* = 296.28 to 307.75°, which agree with a previous report that indicate that peonidin was stable up to pH 8 (Rajan et al., 2018). For solutions with pH 8, the $t_{80\%}$ (time to change 20 % of the original *Hue*) values were in the range 41 – 71 min. However, for solutions with pH 4 and 10, the $t_{80\%}$ values were higher. The increase in temperature reduced the stability of pigments, increasing the value of *k* (resulting in color change, Fig. 3b, Table 2). In general, the $t_{80\%}$ values were decreasing as function of the temperature. Shorter times were achieved in solutions treated at 80 °C; on the contrary, lower temperatures increase $t_{80\%}$ values.

Regarding E_a, it should be noted that E_a increased for solutions with pH 4 and 10. These two conditions had the highest stability for treatments at 40 °C and shoed the lowest *k* values. As can be seen in Fig. 3b (red and blue dots), greater E_a values means greater sensitivity to heat (Ahmed et al., 2002). For solution with pHs 2 and 12, the E_a values were 58.70 and 45.35 kJ/mol, respectively. E_a values were higher for solutions with pH 8 and lower for solution with pHs 4 and 10. High *k* values indicate a rapid color change; in this case, faster anthocyanin degradation. On the contrary, low E_a values were obtained for the solution with pH 8; this indicates that this solution was the less heat sensitive. It kept its purple color; therefor, the solution might require more treatment time to observe a change s in color.

E_a values were used for calculating Q_{10} (Table 2). It was observed that Q_{10} values were greater at lower temperatures, contrary to the values observed at elevated temperatures. Particularly, for solutions at pH 4 and 10, the Q_{10} value was high which is in accordance with the E_a value and the high sensitivity to heat. Other authors have mentioned that high E_a and Q_{10} values may indicate a great dependency of temperature for the degradation of anthocyanins (Özkan et al., 2005) which is the case for the color changes in *J. spicigera* extracts. Low Q_{10} values obtained at elevated temperatures might mean that at certain temperatures (around 60 °C) the process will be equivalent at any elevated temperature. This was observed in solutions with for pH 2, 12 and 8. For extracts with pH 8, despites temperatures increase, the color change could be almost the same. On the contrary, for extracts with pH 2 and 12 and low temperature, the color fading would be 2.40 and 2.08 times faster, respectively, when increasing 10 °C (from 40 to 50 °C). For Q_{10}, the change in color could be observed almost at the same time, no matter the temperature. These changes can be associated to the instability of anthocyanins (quinoidal base form) which can undergo opening of rings to deliver yellow chalcones (Rodriguez-Amaya, 2019). Therefore, anthocyanins from *J. spicigera* might be suitable for coloring foods with pH in the range 2 – 8 that are going be submitted to thermal treatments.

3.4. Time-to-Failure: time-viability approach

The Time-to-Failure model was used to describe the influence of pH and temperature on the stability of color of *J. spicigera* pigments. Two parameters were selected as possible color descriptors for color changes due to the thermal treatment (thermal sensitivity). Total color difference (ΔE) is a well-known parameter that relates the differences of color between two situations (initial to final, initial to any time or initial and after some physical or chemical change). Total color differences greater than 4 could be distinguish by the naked human eye (Krieger et al., 2020). This value was "set as a failure" for the thermal treatment. On the other hand, the Hue_{20} ($\leq$20 %) value denotes the hue of a color; however, there has not been established a particular value for relating changes in *Hue* to a perceptible change in color to the human naked eye.

Table 2
Kinetic parameters for thermal degradation of *Justicia spicigera* natural pigments at different pH.

pH	T(°C)	*k* (min $^{-1}$)	$T_{80\%}$ (min)	R^2	*Ea* (kJ/mol)	$K_{40\text{-}50}$	$Q_{10\ (40\rightarrow50)}$	$k_{60\text{-}70}$	$Q_{10\ (60\rightarrow70)}$
	40	0.0025	88.21	0.891					
2	60	0.0176	12.68	0.997	58.70	0.006	2.40	0.022	1.23
	80	0.0318	7.03	0.996					
	40	0.0001	1544.59	0.011					
4	60	0.0022	101.33	0.987	90.27	0.001	3.54	0.004	1.65
	80	0.0071	31.24	0.994					
	40	0.0031	71.96	0.962					
8	60	0.0041	54.96	0.975	12.83	0.004	1.15	0.005	1.16
	80	0.0054	41.14	0.965					
	40	1.2×10^{-5}	19100.83	0.224					
10	60	0.0009	235.48	0.966	154.99	0.000	7.99	0.003	2.85
	80	0.0096	23.30	0.952					
	40	0.0079	28.32	0.979					
12	60	0.0421	5.30	0.998	45.35	0.016	2.08	0.044	1.04
	80	0.0552	4.04	0.999					

* Kinetic parameters were not calculated because no differences in color were observed.

Therefore, a change greater than 20 %, which is equivalent to a change in 36° (considering 180° as 100 %), was used as a "failure value" for the TTF model. Values of both ΔE and *Hue* are listed in Table S2. It can be observed that the Time-to-Failure value decreases as pH increases. The instability of anthocyanins in the *J. spicigera* extracts has already been discussed in previous sections. In general, the time to achieve a failure coincide for both ΔE and *Hue*; mainly, nearby neutral pH values which are the more stable solutions (Table 2).

Two equations (14, 15) were obtained to describe each parameter as function of TTF.

$$Ln(TTF\Delta E) = 7.362 - 0.995pH + 0.002T - 0.323pH \times T - 0.828pH^2 - 0.190T^2 \quad (14)$$

$$Ln(TTFHue_{20}) = 7.317 - 0.801pH - 0.303T + 0.167pH \times T - 1.304pH^2 + 0.004T^2 \quad (15)$$

The accuracies (R^2) for the models were 0.983 and 0.700 for equation (14) and (15), respectively. The equations allow to estimate of effects of temperatures and pH on the pigment's viability time. This means that the probabilistic models could be used to predict the changes that may occur in food matrixes such as pigments. Therefore, this methodology can be used for estimating the failure time of other ingredients in food systems.

Fig. 4 show the Time-to-Failure for changes in ΔE and Hue_{20}, respectively. It can be observed in Fig. 3a an "unstable zone", when temperature increases, causing a change in color ($\Delta E \geq 4$). In this zone, all pigments could be damaged changing their color. Above 150 °C, the color might remain unchanged over 60 min for solutions with pH 2 and 4. As pH increases, lower temperatures are required to reduce their effect on the solutions and maintain the color. ΔE and Hue_{20} of solutions at all pHs, except 12, can be found in the stability zone; however, depending on temperature, the color might be maintained for up to 420 min which could be important in process that involve the use of pigments.

On the other hand, high values in pH in the quadratic term in Eq. (15) increases the curvature of the plot forming a parabola (Fig. 4b). Values of solution at pH 8 were stable for 420 min (the longest time evaluated) at around 130 °C. Over 100 °C in solutions with for pH 4 until 10, the values fall within the stability zone. As a result, very long times, at a fixed temperature, could lead to the pigments degradation; therefore, changes in color (*Hue*) of the foods system.

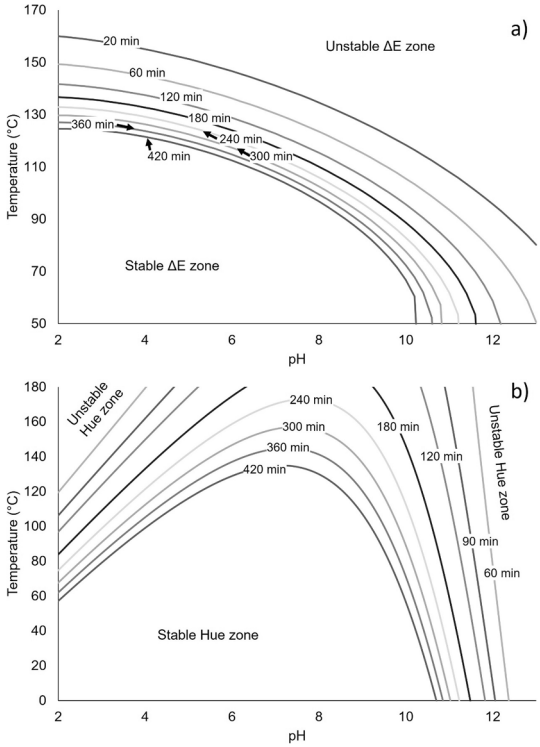

Fig. 4. Time-to-Failure: a) for visual color change (ΔE) and b) for color tone changes (Hue_{20}) of *Justicia spicigera* pigments for different combination of pH and temperature.

4. Conclusions

Justicia spicigera pigments could be used in a variety of foods systems due to their wide range of colors at different pHs. The color of *J. spicigera* extracts or powders in solution may turn into orange, pale-red, purple, and blue from low to high pH. The color changes are mainly due to changes in the molecular structure of anthocyanins in the extract. The thermal treatment affected the color stability; however, it was improved when the treatment was below 60 °C. At pH up to 10, the solutions presented the highest rate color changes. The Time-to-Failure approach was used for evaluating the pigments stability, being a useful tool to determine the stability of color due to thermal treatment. The conditions outside of the stability zone of the temperature vs pH modeling should be avoided to ensure that no color changes in ΔE and *Hue* may occur in the solutions of *J. spicigera*. Depending on the pH and treatment time, a selected temperature could be used for ensuring a desirable final color in the solutions of *J. spicigera* or even in food systems. More complex or more robust models could be used and or include other color parameters for stablishing visual differences by the human naked eye. Evaluation, during food processing, using *J. spicigera* pigments must be done since other coloring compounds in the food system could improve or decrease the color stability. Data obtained in this study could be a useful tool to guide to food producers about the use of natural pigments in food systems.

Author contributions

All authors contribute to design and plan the experiments. To make the technical part (measurements, procedure, and analysis). Draft the manuscript including the design of Figures and Tables. All authors discuss the results and write the manuscript.

Ethical approval/patient consent

This manuscript does not contain any studies with human participants or animals performed by any of the authors. Ethics approval or patient consent was not required for this study.

Declaration of Competing Interest

The authors declare that they have no known competing financial interests or personal relationships that could have appeared to influence the work reported in this paper.

Data availability

Data will be made available on request.

Acknowledgments

Author Jiménez-González thanks to the Universidad de las Americas Puebla (UDLAP) and the National Council for Science and Technology (CONACyT) of Mexico for the financial support for his PhD studies.

Appendix A. Supplementary data

Supplementary data to this article can be found online at https://doi.

org/10.1016/j.fochms.2022.100158.

References

Ahmed, J., Shivhare, U. S., & Sandhu, K. S. (2002). Thermal degradation kinetics of carotenoids and visual color of papaya puree. *Journal of Food Science, 67*(7), 2692–2695. https://doi.org/10.1111/j.1365-2621.2002.tb08800.x

Alvarez-Poblano, L., Roman-Guerrero, A., Vernon-Carter, E. J., & Alvarez-Ramirez, J. (2020). Exogenous addition of muicle (*Justicia spicigera* Schechtendal) extract to white maize tortillas affects the antioxidant activity, texture, color, and in vitro starch digestibility. *LWT, 133*, Article 110120. https://doi.org/10.1016/j.lwt.2020.110120

APHA, (American Public Health Association), AWWA, (American Water Works Association), & WEF, (Water Environment Federation). (1992). 2120 COLOR. In M. A. H. Franson (Ed.), *Standard methods for the examination of water and wastewater* (18th ed., Vol. 1–0). American Public Health Association. 10.2105/SMWW.2882.017.

Awad, N. E., Abdelkawy, M. A., Hamed, M. A., Souleman, A. M. A., Abdelrahman, E. H., & Ramadan, N. S. (2015). Antioxidant and hepatoprotective effects of Justicia spicigera ethyl acetate fraction and characterization of its anthocyanin content. *International Journal of Pharmacy and Pharmaceutical Sciences, 7*(8), 91–96.

Baqueiro-Peña, I., & Guerrero-Beltrán, J.Á. (2017). Physicochemical and antioxidant characterization of *Justicia spicigera*. *Food Chemistry, 218*, 305–312. https://doi.org/10.1016/j.foodchem.2016.09.078

Cabrita, L., Fossen, T., & Andersen, Ø. M. (2000). Colour and stability of the six common anthocyanidin 3-glucosides in aqueous solutions. *Food Chemistry, 68*(1), 101–107. https://doi.org/10.1016/S0308-8146(99)00170-3

Cantrell, K., Erenas, M. M., de Orbe-Payá, I., & Capitán-Vallvey, L. F. (2010). Use of the Hue parameter of the Hue, saturation, value color space as a quantitative analytical parameter for bitonal optical sensors. *Analytical Chemistry, 82*(2), 531–542. https://doi.org/10.1021/ac901753c

Castro-Alatorre, N. C., Gallardo-Velázquez, T., Boyano-Orozco, L. C., Téllez-Medina, D. I., Meza-Márquez, O. G., & Osorio-Revilla, G. (2021). Extraction and microencapsulation of bioactive compounds from muicle (*Justicia spicigera*) and their use in the formulation of functional foods. *Foods, 10*(8), 1747. https://doi.org/10.3390/foods10081747

Cevallos-Casals, B. A., & Cisneros-Zevallos, L. (2004). Stability of anthocyanin-based aqueous extracts of Andean purple corn and red-fleshed sweet potato compared to synthetic and natural colorants. *Food Chemistry, 86*(1), 69–77. https://doi.org/10.1016/j.foodchem.2003.08.011

da Silva Simão, R., de Moraes, J. O., Lopes, J. B., Frabetti, A. C. C., Carciofi, B. A. M., & Laurindo, J. B. (2022). Survival analysis to predict how color influences the shelf life of strawberry leather. *Foods, 11*(2), 218. https://doi.org/10.3390/foods11020218

Fossen, T., Cabrita, L., & Andersen, O. M. (1998). Colour and stability of pure anthocyanins influenced by pH including the alkaline region. *Food Chemistry, 63*(4), 435–440. https://doi.org/10.1016/S0308-8146(98)00065-X

Gacula, M. C., & Singh, J. (1984). *Statistical Methods in Food and Consumer Research*. Academic Press. 10.1016/C2009-0-02978-X.

Gençdağ, E., Özdemir, E. E., Demirci, K., Görgüç, A., & Yılmaz, F. M. (2022). Copigmentation and stabilization of anthocyanins using organic molecules and encapsulation techniques. *Current Plant Biology, 29*, Article 100238. https://doi.org/10.1016/j.cpb.2022.100238

Habtemariam, S. (2019). Bilberries and blueberries as potential modulators of type 2 diabetes and associated diseases. In *Medicinal Foods as Potential Therapies for Type-2 Diabetes and Associated Diseases* (pp. 135–175). Elsevier. https://doi.org/10.1016/B978-0-08-102922-0.00007-9.

Jacobo-Velázquez, D. A., Ramos-Parra, P. A., & Hernández-Brenes, C. (2010). Survival analysis applied to the sensory shelf-life dating of high hydrostatic pressure processed avocado and mango pulps. *Journal of Food Science, 75*(6), S286–S291. https://doi.org/10.1111/j.1750-3841.2010.01656.x

Jiménez-González, O., & Guerrero-Beltrán, J.Á. (2022). Microencapsulates by spray of *Lacticaseibacillus rhamnosus* GG from fermented whole or skimmed cow's milk added with Mexican honeysuckle (*Justicia spicigera*) extract using mesquite gum as carrier agent. *Heliyon, 8*(9), e10733.

Khoo, H. E., Azlan, A., Tang, S. T., & Lim, S. M. (2017). Anthocyanidins and anthocyanins: Colored pigments as food, pharmaceutical ingredients, and the potential health benefits. *Food & Nutrition Research, 61*(1), 1361779. https://doi.org/10.1080/16546628.2017.1361779

Kosegarten, C. E., Ramírez-Corona, N., López-Malo, A., & Mani-López, E. (2022). Wheat-based fried snacks shelf-life prediction using kinetic, probabilistic, and time-to-fail models. *Journal of Food Processing and Preservation*. https://doi.org/10.1111/jfpp.16548

Kosegarten, C. E., Ramírez-Corona, N., Mani-López, E., Palou, E., & López-Malo, A. (2017). Description of *Aspergillus flavus* growth under the influence of different factors (water activity, incubation temperature, protein and fat concentration, pH, and cinnamon essential oil concentration) by kinetic, probability of growth, and time-to-detection models. *International Journal of Food Microbiology, 240*, 115–123. https://doi.org/10.1016/j.ijfoodmicro.2016.04.024

Krieger, L. W. M. M., Ridge, T., Demers, A., Vishwanath, K., & Sparks, J. L. (2020). Method for improving skin color accuracy of three-dimensional printed training models for early pressure ulcer recognition. In *Innovations and Emerging Technologies in Wound Care* (pp. 245–279). Elsevier. https://doi.org/10.1016/B978-0-12-815028-3.00014-6.

Liao, M., Zou, B., Chen, J., Yao, Z., Huang, L., Luo, Z., & Wang, Z. (2019). Effect of domestic cooking methods on the anthocyanins and antioxidant activity of deeply purple-fleshed sweetpotato GZ9. *Heliyon, 5*(4), e01515.

Loypimai, P., Moongngarm, A., & Chottanom, P. (2016). Thermal and pH degradation kinetics of anthocyanins in natural food colorant prepared from black rice bran. *Journal of Food Science and Technology, 53*(1), 461–470. https://doi.org/10.1007/s13197-015-2002-1

Marques, C., Lise, C. C., de Lima, V. A., & Daltoé, M. L. M. (2020). Survival analysis and cut-off point to estimate the shelf life of refrigerated fish burgers. *Food Science and Technology, 40*(1), 171–177. https://doi.org/10.1590/fst.36918

Moreno, J., & Peinado. (2012). Polyphenols. In *Enological Chemistry* (pp. 53–76). Elsevier. https://doi.org/10.1016/B978-0-12-388438-1.00005-4.

Muche, B. M., Speers, R. A., & Rupasinghe, H. P. V. (2018). Storage temperature impacts on anthocyanins degradation, color changes and haze development in juice of "Merlot" and "Ruby" grapes (*Vitis vinifera*). *Frontiers in Nutrition, 5*, 100. https://doi.org/10.3389/fnut.2018.00100

Ngamwonglumlert, L., Devahastin, S., Chiewchan, N., & Raghavan, G. S. V. (2020). Color and molecular structure alterations of brazilein extracted from *Caesalpinia sappan* L. under different pH and heating conditions. *Scientific Reports, 10*(1), 12386. https://doi.org/10.1038/s41598-020-69189-3

Oancea, S. (2021). A Review of the current knowledge of thermal stability of anthocyanins and approaches to their stabilization to heat. *Antioxidants, 10*(9), 1337. https://doi.org/10.3390/antiox10091337

Özkan, M., Yemenicioğlu, A., & Cemeroğlu, B. (2005). Degradation of various fruit juice anthocyanins by hydrogen peroxide. *Food Research International, 38*(8–9), 1015–1021. https://doi.org/10.1016/j.foodres.2005.03.013

Patras, A., Brunton, Nigel, P., O'Donnell, C., & Tiwari, B. K. (2010). Effect of thermal processing on anthocyanin stability in foods; mechanisms and kinetics of degradation. *Trends in Food Science & Technology, 21*(1), 3–11. https://doi.org/10.1016/j.tifs.2009.07.004

Rajan, V. K., Shameera Ahamed, T. K., Hasna, C. K., & Muraleedharan, K. (2018). A non toxic natural food colorant and antioxidant 'Peonidin' as a pH indicator: A TDDFT analysis. *Computational Biology and Chemistry, 76*, 202–209. https://doi.org/10.1016/j.compbiolchem.2018.07.015

Rakić, V., & Poklar Ulrih, N. (2021). Influence of pH on color variation and stability of cyanidin and cyanidin 3- *O*-β -glucopyranoside in aqueous solution. *CyTA - Journal of Food, 19*(1), 174–182. https://doi.org/10.1080/19476337.2021.1874539

Rasane, P., Jha, A., & Sharma, N. (2015). Predictive modelling for shelf life determination of nutricereal based fermented baby food. *Journal of Food Science and Technology, 52*(8), 5003–5011. https://doi.org/10.1007/s13197-014-1545-x

Rodriguez-Amaya, D. B. (2016). Natural food pigments and colorants. *Current Opinion in Food Science, 7*, 20–26. https://doi.org/10.1016/j.cofs.2015.08.004

Rodriguez-Amaya, D. B. (2019). Update on natural food pigments—A mini-review on carotenoids, anthocyanins, and betalains. *Food Research International, 124*, 200–205. https://doi.org/10.1016/j.foodres.2018.05.028

Roobha, J. J., Saravanakumar, M., Aravindhan, K. M., & Devi, P. S. (2011). The effect of light, temperature, pH on stability of anthocyanin pigments in Musa acuminata bract. *Research in Plant Biology*, *1*(5), Article 5. https://updatepublishing.com/journal/index.php/ripb/article/view/2597.

Sadilova, E., Stintzing, F. C., & Carle, R. (2006). Thermal degradation of acylated and nonacylated anthocyanins. *Journal of Food Science, 71*(8), C504–C512. https://doi.org/10.1111/j.1750-3841.2006.00148.x

Shannon, E., Jaiswal, A. K., & Abu-Ghannam, N. (2017). Polyphenolic content and antioxidant capacity of white, green, black, and herbal teas: A kinetic study. *Food Research*, *2*(1), 1–11. 10.26656/fr.2017.2(1).117.

Speers, R. A., Tung, M. A., & Jackman, R. L. (1987). Prediction of Colour Deterioration in Strawberry Juice. *Canadian Institute of Food Science and Technology Journal, 20*(1), 15–18. https://doi.org/10.1016/S0315-5463(87)70663-4

Swain, S., Samuel, D. V. K., Bal, L. M., & Kar, A. (2014). Thermal kinetics of colour degradation of yellow sweet pepper (*Capsicum Annum* L.) undergoing microwave assisted convective drying. *International Journal of Food Properties, 17*(9), 1946–1964. https://doi.org/10.1080/10942912.2013.775150

Zhai, L.-Y., Lu, W.-F., Liu, Y., Li, X., & Vachtsevanos, G. (2013). Analysis of Time-to-Failure data with Weibull model in product life cycle management. In A. Y. C. Nee, B. Song, & S.-K. Ong (Eds.), *Re-engineering Manufacturing for Sustainability* (pp. 699–703). Springer. https://doi.org/10.1007/978-981-4451-48-2_114.